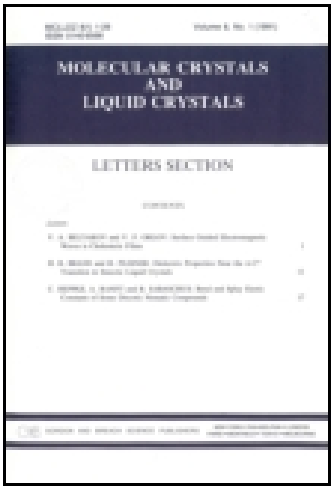

Molecular Crystals and Liquid Crystals
Publication details, including instructions for authors and subscription information:
http://www.tandfonline.com/loi/gmcl20

Local Optical Spectra and Texture for Chiral Nematic Liquid Crystals in Cells with Interdigitated Electrodes

Mariacristina Rumi[ab], Vincent P. Tondiglia[ac], Lalgudi V. Natarajan[ac], Timothy J. White[a] & Timothy J. Bunning[a]

[a] Materials and Manufacturing Directorate, Air Force Research Laboratory, Wright Patterson Air Force Base, OH, USA

[b] Azimuth Corporation, Dayton, OH, USA

[c] Science Applications International Corporation, Beavercreek, OH, USA

Published online: 30 Sep 2014.

To cite this article: Mariacristina Rumi, Vincent P. Tondiglia, Lalgudi V. Natarajan, Timothy J. White & Timothy J. Bunning (2014) Local Optical Spectra and Texture for Chiral Nematic Liquid Crystals in Cells with Interdigitated Electrodes, Molecular Crystals and Liquid Crystals, 595:1, 123-135, DOI: 10.1080/15421406.2014.917825

To link to this article: http://dx.doi.org/10.1080/15421406.2014.917825

Mol. Cryst. and Liq. Cryst., Vol. 595: pp. 123–135, 2014

ISSN: 1542-1406 print/1563-5287 online
DOI: 10.1080/15421406.2014.917825

Taylor & Francis
Taylor & Francis Group

Local Optical Spectra and Texture for Chiral Nematic Liquid Crystals in Cells with Interdigitated Electrodes

MARIACRISTINA RUMI,[1,2] VINCENT P. TONDIGLIA,[1,3] LALGUDI V. NATARAJAN,[1,3] TIMOTHY J. WHITE,[1] AND TIMOTHY J. BUNNING[1,*]

[1]Materials and Manufacturing Directorate, Air Force Research Laboratory, Wright Patterson Air Force Base, OH, USA
[2]Azimuth Corporation, Dayton, OH, USA
[3]Science Applications International Corporation, Beavercreek, OH, USA

A microspectrophotometer was used to measure reflection spectra of cholesteric liquid crystals (CLCs) in cells with interdigitated electrodes as a function of applied voltage in order to probe the spatial variation in behavior in the electrode and gap regions. Complex changes in the optical spectra are observed in the gap regions for cells in which the electric field magnitude changes significantly through the thickness of the cell. This leads to a non-uniform helix unwinding and pitch gradient in the cell. In cells with smaller field gradients, the unwinding occurs in a uniform manner and it is possible, under certain conditions, to distinguish discrete changes in pitch, corresponding to a decrease in the number of half-turns of the helical structure in the cell.

Keywords Cholesteric liquid crystals; interdigitated electrodes; helix unwinding; microspectrometer

Introduction

Cells with interdigitated electrodes (IDEs) have often been used to generate electric fields directed parallel to the cell substrate. A chiral nematic liquid crystal with positive dielectric anisotropy and helical axis directed perpendicular to the substrate can undergo a progressive unwinding and deformation of the helical structure in such an electric field, which results in a red-shift of the Bragg reflection peak [1–4]. However, the field direction and magnitude are not uniform in this type of cell [5]. When a potential difference is applied between the two sets of electrodes in IDE cells, the electric field in the center of the gap region is parallel to the plane of the substrate and perpendicular to the electrode length, whereas the field in the center of each electrode pad is perpendicular to the substrate. The field direction changes continuously from parallel to perpendicular to the substrates between the gap center and the electrode center and thus there should be a spatial variation of the optical response. In addition, the electric field distribution is different depending on the cell

*Address correspondence to Timothy J. Bunning, Materials and Manufacturing Directorate, Air Force Research Laboratory, Wright Patterson Air Force Base, OH 45433, USA. E-mail: timothy.bunning@us.af.mil

parameters [6] and CLC devices in IDE cells can manifest different optical responses to electric fields depending on geometry. An investigation using cells with various electrode dimensions should provide a more detailed understanding of the helix behavior in an electric field.

We are particularly interested in the local variations in the helical structure in the gap regions of the IDE cells, as opposed to the macroscopic response of the devices, which is an average over both electrode and gap regions. As the effective area of the regions with field parallel to the cell substrate depends on electrode parameters, the average response should scale accordingly. However, it has not yet been fully explored if changes in the intrinsic response of the material to electric fields may also be present or what is the maximum achievable reflectance for various degrees of deformation of the cholesteric helix.

In our current investigation a microspectrophotometer was used to probe sample areas small with respect to the dimensions of the electrode pattern. This technique allows us to separate the contributions to the optical response coming from the electrode and gap regions of the cell, as well as the transition regions between them. Here we will discuss only spectral data obtained when probing the center of gap regions, where the field is parallel to the substrate and where the helical structure should unwind and become deformed when the electric field is present. The results presented here and in another recent publication of ours [7] indicate that complex changes in the optical spectra are observed even in the gap regions in cells with relatively narrow spacing between electrodes, because the electric field-induced helix unwinding can occur in a non-uniform manner, due to variations in electric field magnitude through the thickness of the cell. When the electrode spacing is wider and the cell is sufficiently thin, however, the electric field is approximately constant in the thickness direction at the center of the gap and the red-shift of the reflection notch with increasing electric field strength follows the expected trend. We will show that for certain CLC mixtures, the change in pitch occurs in discrete steps each corresponding to unwinding by half of the helix period and that the efficiency of the Bragg reflection remains high even for a strongly deformed helix.

Experimental Details

IDE cells with the following characteristics were used:

Type-I cell: $w = 15\ \mu$m, $d = 15\ \mu$m, $L = 8.8$–$9.1\ \mu$m;
Type-II cell: $w = 56\ \mu$m, $d = 44\ \mu$m, $L = 4.7$–$5.0\ \mu$m,

where w is the width of each electrode pad, d the distance between electrodes (gap), and L is the cell thickness. In these cells, two sets of linear and parallel electrodes are patterned in the ITO layer on one of the substrates. The other substrate is uniform glass (no ITO). Cells of type I were purchased from Instec (model IPS02A088uX000) and cells of type II were kindly provided by Prof. Deng-Ke Yang, Kent State University. In all the IDE cells, the top and bottom substrates of the cell were coated with polyimide and the rubbing direction was parallel to the electrodes. The cells were filled by capillary action while heated on a hot plate set slightly above the clearing temperature of the mixtures.

The CLC mixture used for this investigation consisted of 4–5% R1011 (chiral dopant) in the nematic host BL037. The materials were obtained from Merck and used as received. According to the Merck specification sheet, the dielectric anisotropy of BL037 is $\Delta\varepsilon = +15.9$

at 1 kHz, the ordinary refractive index n_o is 1.526 at 589 nm and the birefringence at the same wavelength is $\Delta n = 0.282$.

The electric field was applied as a square wave at 1 kHz using a function generator (Agilent, model 33120A) and an amplifier (MTS, model M94100). The values reported in the text are quoted as root-mean-square (rms) numbers for both potential difference and electric field. Reflection spectra of the samples in IDE cells were obtained on a microspectrophotometer (CRAIC Technologies, model MSP 121) using a 36X objective and a sampling spot size of ca. $4 \times 4\ \mu m^2$, averaging at least 10 acquisition per spectrum. Natural light was used in all cases. The data are reported relative to an aluminum mirror, which was used as a reference under the same illumination and collection conditions as the samples. A variation in light intensity delivered and collected by the objective for sample distances that yield images equally well focused was a source of uncertainty for the reflectance measurements and as such reflectance values obtained in independent measurements were found to differ by a few percent points. Spectra obtained in the same measurement session, during which the sample height was not varied, had better instrumental repeatability and observed differences represent actual variations in materials properties.

Results and Discussion

The electrode dimensions and cell thickness for type-II cells are similar to those used in two of previous studies on the effect of an in-plane electric field on the cholesteric pitch [1, 2]. Cells of type-I are thicker and have narrower electrodes and gaps than type-II cells. We have calculated that the electric field magnitude at the center of the gaps in type-I cells decreases significantly, by about 50%, from the side of the patterned substrate to the opposite, uniform substrate of the cell. In contrast, the electric field is almost constant in magnitude through the thickness of the cell in the type-II case. We have also shown that the reflection spectra of CLC mixtures in type-I cells can display a complex behavior as a function of applied electric field [7].

Here we present an additional example of the effect of electric fields directed perpendicular to the helical axis and how the corresponding changes in Bragg reflection differ in type-I and type-II cells. The Bragg reflection of the starting material, a BL037/R1011 mixture, is centered at 900–910 nm. As voltage was applied in a type-I cell (Fig. 1), the reflection band first underwent a broadening on the long wavelength side and at higher voltages a shoulder or separate peak developed on the long wavelength side of the band, whose position appeared to red-shift with increasing voltage up to about 80 V. However, the details of the shape and the relative intensities of the original band and the red-shifted peak or shoulder depend on the side of the sample from which the reflection was collected. For example, the long wavelength side of the band was often more intense for spectra obtained from the patterned side (Fig. 1a) than from the uniform side of the cell (Fig. 1b). From 90 V upward, the reflection band was observed at a wavelength close to that for zero field, p_0, or slightly shorter, and the band position was similar from both sides of illumination. There also seemed to be a significant decrease in the maximum reflectance in this voltage range (especially in the case shown in Fig. 1a). It should be mentioned that we observed a relatively large variation of reflectance magnitudes for repeated measurements on the same location or between nearby locations, all at gap centers, for this sample. The variation is probably due to the presence of defects that moved over time over the measurement spots. The shape of the measured spectrum represents, effectively, the sum of spectra of the various domains that exist at the measurement spot during the collection time. The magnitude of the reflectance could also be affected by the speed with which defects flowed

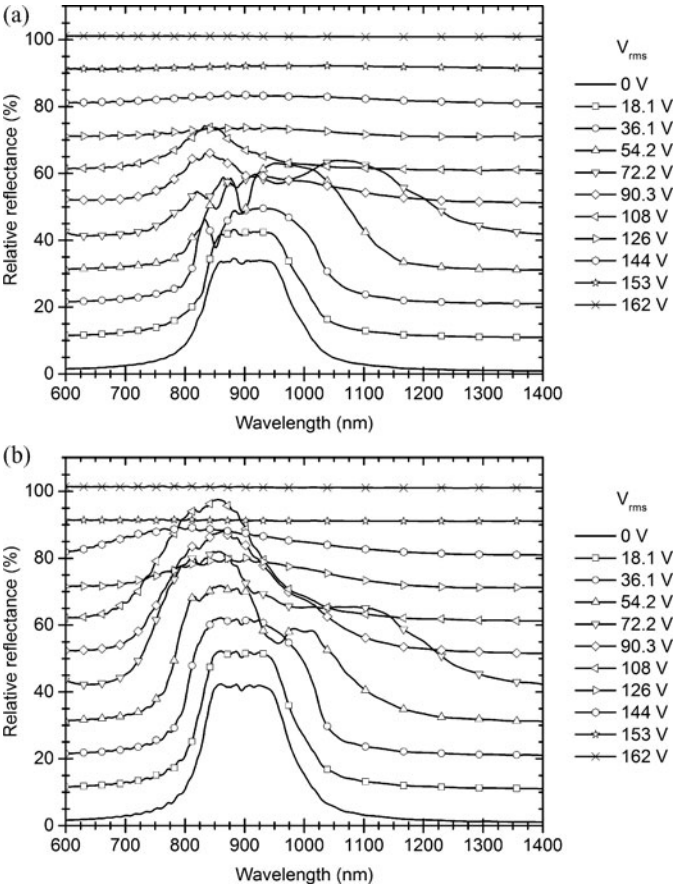

Figure 1. Reflection spectra of a BL037/R1011 mixture in a type-I cell at the center of gap regions as a function of applied voltage. The sample was illuminated and the reflection was collected from (a) the patterned side and (b) the uniform side of the cell. Each spectrum is shifted by 10 units on the reflectance scale for clarity between 0 and 162 V.

thought the gap region, as a defect with low or no reflectance would decrease the effective reflectance measured at a given location.

We have also considered different CLC mixtures with respect to that studied in Fig. 1 and found that the general behavior of complex changes in optical spectra with increasing voltage and asymmetry in the response from the two sides of the cell is the same. This suggests that the observed behavior is consistent for different compositions and supports the interpretation that the large variation in electric field in the gap center of type-I cells is responsible for a non-uniform unwinding of the helix and the formation of a pitch gradient or graded structure at intermediate electric field strengths.

If the electric field were constant as a function of height in the cell, the notch position should change with applied voltage according to the solid dark line in Fig. 2. This was obtained by minimizing the energy density of the system in the presence of a field following the approach described by de Gennes [8] (see also Refs. [9] and [2]). It can be seen that below 80–90 V this line describes approximately the evolution of the long-wavelength side of the Bragg reflection. In this voltage range, the electric field is large enough to affect the

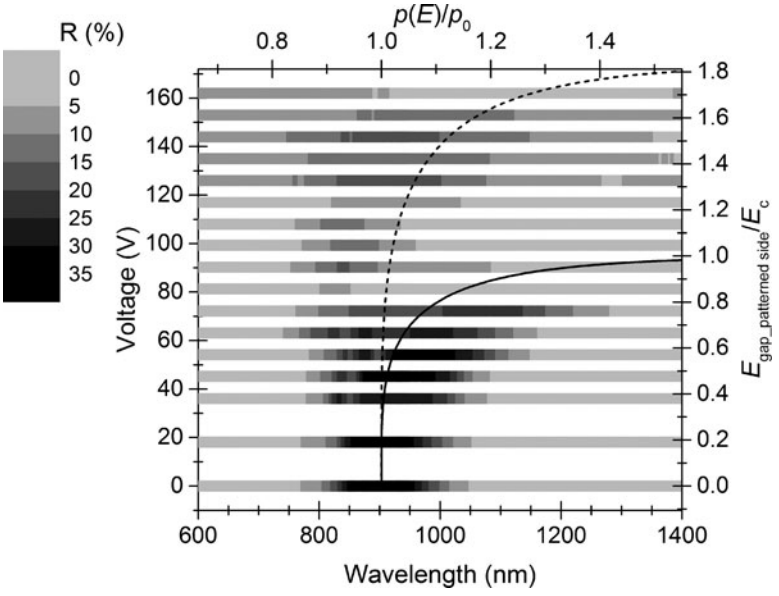

Figure 2. Left and bottom axis: Reflectance values for the BL037/R1011 mixture in a type-I cell at the center of the gap as a function of voltage and wavelength, collected from the patterned side of the cell. The data on any horizontal strip are from a single spectrum at a fixed voltage (for display purposes, the strips have finite thickness around the actual voltage value) and the strip colors at various wavelengths represent the measured reflectance values. This is the same data set displayed in Fig. 1a, but all the tested voltage values are shown. For $V < 120$ V, the reflectance color scale is given on the left side of the graph; for $V > 120$ V, the trace colors correspond to the measured reflectance multiplied by five. Each spectrum is displaced vertically by an amount proportional to the applied voltage (left axis). Top and right axis: expected variation of pitch with electric field based on theory, relative to p_0. The electric field scale on the right axis is for the values at the center of the gap on the patterned substrate, normalized to E_c. Solid line: pitch variation at height 0 μm in the cell (at the patterned substrate); dashed line: pitch variation at height 9 μm in the cell (at the uniform substrate).

helical pitch only in a thin layer of material close to the patterned substrate; this part of the CLC thus exhibits a longer wavelength reflection than the rest of the sample. Thus, the solid line in Fig. 2 represents the pitch evolution of the CLC layer at the patterned substrate side of the cell. The longer wavelength reflection appears stronger when the spectra are collected from the patterned side of the cell than from the uniform side (Fig. 1). Around 90 V, the field in this layer is close to E_c, the critical electric field [9] at which the system loses the helical structure (the pitch diverges to infinity). Once this layer undergoes the cholesteric to nematic transition, it no longer contributes to the reflection of the cell and thus the spectra do not have a long-wavelength peak or shoulder (Fig. 2). Above 100 V, the electric field is sufficiently large in the middle layers of the cell to induce some pitch elongation there. However, if these layers are relatively thin, their efficiency for Bragg reflection is low and they do not contribute significantly to the overall reflection spectrum of the sample, which is now dominated by the CLC layer closest to the uniform substrate and where the field is still small with respect to E_c. This explains why in this intermediate field regime, the reflection band is observed close to the pristine value (the blue shift observed in some cases could be due to a small tilting of the helix axis). According to preliminary estimates of the electric field at the center of the gaps in a type-I cell, the field strength near the uniform substrate

side of the cell should be 54% of the value near the patterned side, for any fixed applied voltage. The pitch change of the CLC in this part of the cell is represented by the dashed line in Fig. 2. The pitch for all other layers of the cell should be between the two points at which the solid and dashed curves intersect a constant voltage (horizontal) line below E_c or to the right side of the dashed line above E_c. Thus, we would expect some progressive increase in notch position above 120–140 V, where the dashed line starts deviating significantly from p_0. This red-shift, though, is not conclusively observed experimentally in the case shown in Fig. 1 and 2, probably because the number of repeat units of the helical structure in this layer is small for this long-pitch sample. We should mention, however, that a small red-shift in the high-voltage regime was observed for a different sample, a BL038/CB15 mixture with notch around 500 nm, on which we will report separately. It is also possible that the final red-shift before the cholesteric-nematic transition is masked by the inevitable averaging over defects and multiple domains, as mentioned above. Additional experiments would be required to test these possibilities. For this cell geometry, all layers of the liquid crystal material should be in the nematic phase with the director parallel to the electric field when the field at the uniform substrate reaches E_c, corresponding to about 160 V for this CLC sample (and a field of about 1.8 E_c at the patterned substrate). This is in good agreement with the voltage at which reflectance from the sample is no longer measurable (Fig. 1).

The changes in Bragg reflection position when the same sample is placed in type-II cell are different as the band progressively shifts to longer wavelengths when the applied voltage was increased. This evolution was similar when the spectra were collected from either the patterned or uniform side of the cell. The results for the patterned side are shown in Fig. 3a. At first examination, it appears that there are non-monotonic shifts in the band position, as the notch was observed at a longer wavelength at 170 V than either 152 or 179 V. However, this is simply due to the fact that multiple domains with different pitches were present in the sample once changes started to occur at finite electric field values. One example in which three domains with measurably different pitches were observed in a small sample area is shown in Fig. 3b.

Spot to spot variations have been seen in all samples and in both cell types, but in the case of type-I cells, these variations could not account for the asymmetry with respect to the illumination side and the negligible changes in the position of the short-wavelength edge of the reflection notch. For the BL037/R1011 sample in type-II cells, once the spatial variations are taken into consideration, the pitch exhibits the expected progressive increase with increasing voltage. This can be clearly seen in Fig. 4a, where the position of the rising and falling edges of the reflection notch for all the measured spectra are shown as a function of applied voltage. The change in the position of the band center is overlaid with the theoretical prediction in Fig. 4b, where we have set the position of the vertical asymptote (dotted line) to correspond to the first voltage value for which no reflection band was observed, 263 V. It should be mentioned that above 240 V, the main reflection band is outside the detector range (above 1700 nm) and thus no data points are included in the graphs in this voltage range. However, up to 263 V, higher order reflection bands are observed elsewhere in the spectrum and indicate that the transition to the nematic state has not yet occurred. The conditions under which high-order modes are observed and their behavior as a function of applied voltage are the subject of an ongoing investigation and will be reported separately.

The difference in initial Bragg reflection for the experiments with type-I (Fig. 1) and type II (Fig. 3a) cells is due to a small variation in composition of the mixtures, which contained about 5% of R1011 in the former and 4% R1011 in the latter case. Because E_c does not depend on the cell geometry and $E_c p_0$ depends only on the elastic constant K_{22} of

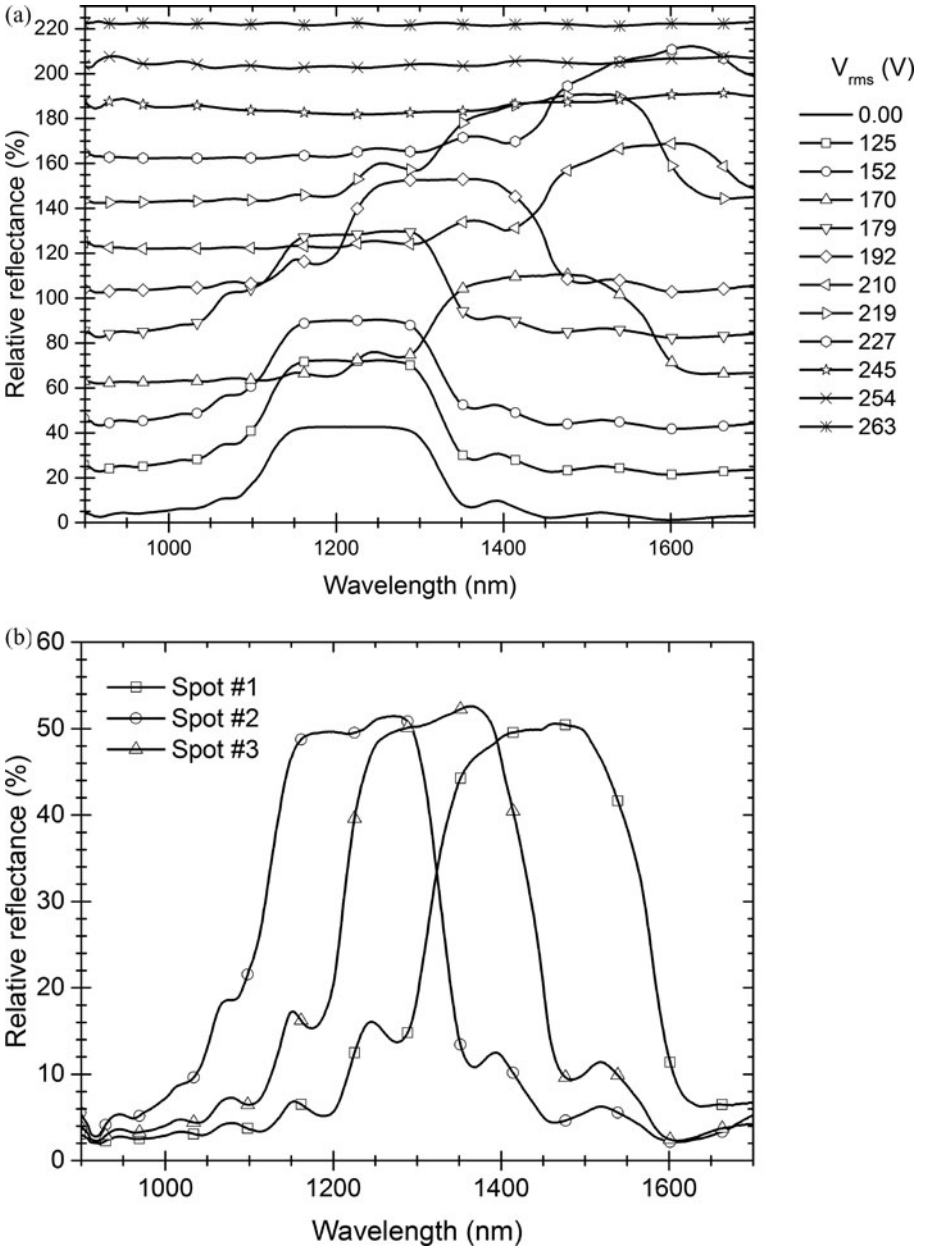

Figure 3. a) Reflection spectra of a BL037/R1011 mixture in a type-II cell at the center of gap regions as a function of applied voltage. The spectra are shifted by 20 units on the reflectance scale for clarity between 0 and 263 V. The spectra were collected in the same location. (b) Reflection spectra for the same sample at 170 V collected in three different locations at the center of gap regions within a 200 μm area. The sample was illuminated and the reflection was collected from the patterned side in all cases.

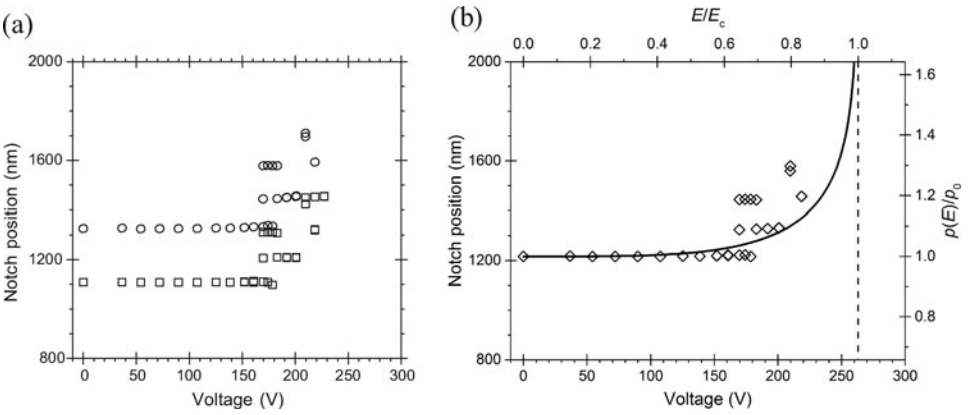

Figure 4. a) Short (squares) and long (circles) wavelength edges of the reflection band of BL037/R1011 as a function of voltage for the type-II case, from the reflection spectra at the center of gap regions collected from the patterned side of the cell. The edge positions were estimated as the half-maximum points on the reflection band. Two or three spectra were collected per voltage value; below 150 V data from different spectra overlap within the symbol edge size. b) Center of reflection notch for the data sets in (a) as a function of applied voltage (left and bottom axes). The dashed line is drawn at the first voltage value for which no reflection band was observed. The theoretical curve (solid line) from the de Gennes model is also displayed (right and top axis) for the relative change in pitch as a function of field strength normalized to E_c, with $E/E_c = 1$ at the dashed line.

the liquid crystal material and its dielectric anisotropy [2, 9], the results from type-II cells can be used to estimate the voltage at which E_c is reached on the patterned side of the cell. Using the value of 263 V to estimate the critical field in type-II cell and accounting for the different gap widths for the two cells and the small variation in p_0 noted above, the critical voltage for type-I cell is found to be about 263 V*(15 μm/56 μm)*(1217 nm/903 nm) = 95 V. This was the value used to set the scale for the right axis in Fig. 2 relative to the left axis and thus it corresponds to the asymptote of the solid curve in that figure.

It can be seen from the data in Fig. 4, that the pitch seems only to assume a discrete set of values when the field electric field is applied to the BL037/R1011 sample in a type-II cell, instead of changing continuously along the simple model curve. Nonetheless, the agreement with the theory is acceptable. The presence of jumps in pitch value for this sample could correspond to variations in the number of half-turns in the helical structure. Indeed, in the case of strong anchoring, as should be true for our samples with rubbed polyimide alignment layers, the orientation of the director should not change near the interfaces, and thus the helical structure should contain an integer number of half periods for all electric field values. Models that include this constraint have been developed [2, 10, 11], but the step-wise change in pitch size has not been observed in IDE cells when an electric field is applied [2]. In Fig. 5, we graphed the observed short-wavelength edge of the reflection band from Fig. 4a in order of increasing wavelength (irrespective of the voltage value at which they are first observed) at regular intervals on the abscissa. The data points for the reflection spectra obtained from the uniform side of the cell are also included in the graph. With zero field, the edge position is given by $\lambda = n_o p_0 = 2n_o L/m$, where n_o is the ordinary refractive index of the LC, L the cell thickness and m an integer. When the field is present, the pitch should increase, but due to the anchoring conditions, the only allowed values for

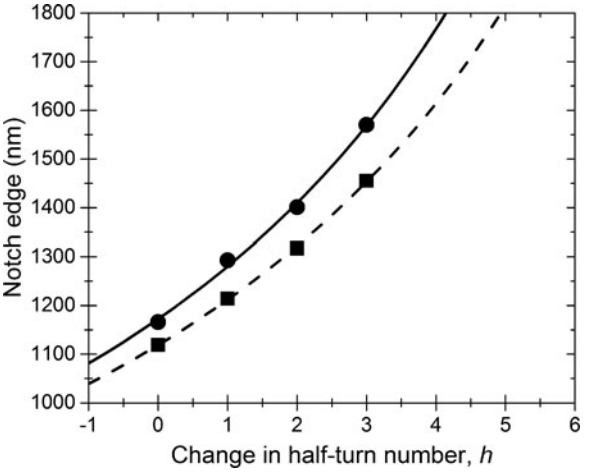

Figure 5. Wavelength at which the short-wavelength edge of the reflection band is observed for voltages between 0 and 140 V in the type-II cell. Squares: reflection data from the patterned side of the cell; circles: reflection data from the uniform side of the cell. The lines are the best fit to Equation (1) with the constraint that m is an integer. The horizontal axis represents the change to m with respect to the case at zero field, i.e. h. Solid line: uniform side; dotted line: patterned side.

the notch edge should be:

$$\lambda = 2n_o L/(m - h) \tag{1}$$

with h also an integer. When we performed a least-square fitting of the data in Fig. 5 to Equation (1), assuming that h counts the observed data points starting at $h = 0$ for the sample at zero field, we obtained the two curves included in the figure. It can be seen that these curves describe well the variation of pitch. The cell thicknesses obtained from the fitting (4.6–4.8 μm) were in good agreement with estimates based on interference fringes of the empty cell (4.9 μm). It should be noted that there is an offset in the notch position in the two data sets included in Fig. 5. This stems from the fact that two distinct sample locations were probed and that the cell had a small wedge. From the fitting, the cell thickness in the two location differed by about 150 nm. The goodness of the fitting results in Fig. 5 suggests that the pitch changes observed in our experiment are indeed due to the variation of the helical structure by half-turn steps. One of the samples discussed by Xianyu et al. [2], a BL087/BL088 mixture, had a Bragg band in approximately the same position as our sample and the cell parameters were very similar. Yet, no discrete changes were observed in that case, and this behavior was attributed to an inhomogeneity of the pitch through the cell thickness, due to the electric field gradient. Also, the peaks did not have steep edges. We attribute the ability to distinguish the discrete changes in half-turn numbers for the BL037/R1011 sample to the spatial selectivity of our measurement, as we are probing only the center of the gap and no other sample regions are contributing to the signal.

The electric field gradient in type-II cell is sufficiently small that the pitch should be effectively the same at all heights in the cell. Yet, we did not observe discrete variations in pitch using a BL038/CB15 mixture in the same type of cell. This could be due to the fact that in other samples more defects were present or domain boundaries moved significantly

during the measurement time, so that many of the collected spectra were effectively averages over multiple domains. In contrast, the results for BL037/R1011 reflect, in most cases, the properties of single domains. At this point, we do not if it is possible to slow the movement of domain boundaries and defects or reduce their number.

All spectra discussed so far were collected at the center of gap regions. It should be mentioned that typically changes in reflection notch position did not occur throughout the gap region at the same voltage. Changes are actually observed at lower voltages toward the edges of the gap, near the electrodes. This is because, for a given applied voltage, the electric field magnitude is larger at the edges of the gap than near the center, so that a gradient of pitches could be present in the plane of the substrate in addition to that through the thickness of the cell. A detailed discussion of this lateral variation of the pitch it outside the scope of this investigation. However, this further illustrates that only probing areas small with respect to the cell pattern it is possible to obtain detailed information on the helix unwinding process and correlate this with specific electric field magnitudes.

The presence of a lateral field gradient allowed the observation of double disclination lines under certain conditions. It can be seen in Fig. 6a that the central part of the gap is separated from the top and bottom parts of the gap by lines with a zigzag shape (the contrast between the two regions in the image is low because of the long pitch for this sample). In the presence of a field, a zigzag line should correspond to the boundary between two domains that differ by a full pitch, if the field is perpendicular to the long direction of the boundary. This has been shown for the case of a CLC material in a Cano wedge and in a magnetic field perpendicular the helical axis and along the wedge direction [11, 12]. In that case, the boundaries were straight lines perpendicular to the thickness gradient in the absence of the field and they buckled into the zigzag shape when the field was turned on. In our case, there are typically no boundaries at zero field, if the cell thickness is uniform, but the boundary lines develop during the helix unwinding process. Single lines, separating regions differing by one half-turn should be stable in a field and remain perpendicular to field direction at all points [11, 12]. At other voltages for the same sample we observed both linear and zigzag domain boundaries, as in the case in Fig. 6b. However, the shape of the boundary between domains was not always well defined and it often contained linear and curved sections, especially near the critical field (Fig. 6c). While we do not have yet enough data to correlate the boundary shape and the change in reflection spectra, and thus pitch changes, the presence of lines of different shapes is consistent with the existence of domains with different pitch in the sample, as we have mentioned above.

For the sample in type-II cell, we also observed that the magnitude of the Bragg reflection remained relatively high up to 200 V (Fig. 7a). For one set of measurements (squares in the figure), the reflectance did not decrease below the value at zero field until about 220 V, corresponding to 0.8 E_c, above which an abrupt decrease was observed (in this voltage range only part of the band is in the range of the detector and thus the results in the figure are to be considered lower limits). This behavior is different from the one observed by Xianyu et al. [2], where a gradual decrease in the efficiency of the reflection was recorded starting around 0.5 E_c. The difference with respect to our results is again attributable to the spatial selectivity of our reflection spectra for the center of the gap. The data in Fig. 7a indicate that a deformed helix is still a relatively efficient photonic band gap. This could be of use in practical devices if a way is found to reduce defects, so that single domains are responsible for the observed properties. Above 150 V, the width of the reflection band started to increase (Fig. 7b). However, most of the band broadening is simply due to the concomitant lengthening of the pitch. Indeed, the relative width of

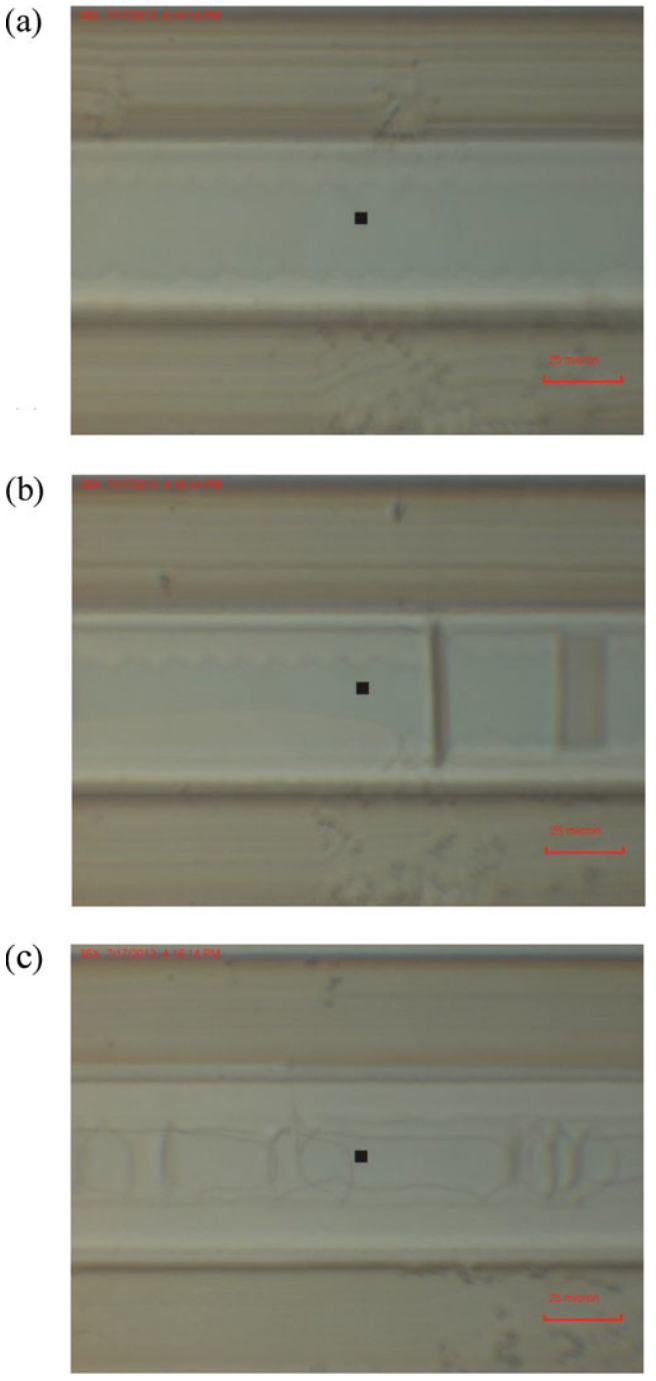

Figure 6. Transmission images obtained during measurements with a microspectrophotometer for the BL037/R1011 sample in a type-II cell: (a) 161 V, (b) 174 V, (c) 241 V. The central portion of the images is a gap region; the top and bottom sections are two electrodes. Size of imaged region: 185 μm $\times$ 140 μm.

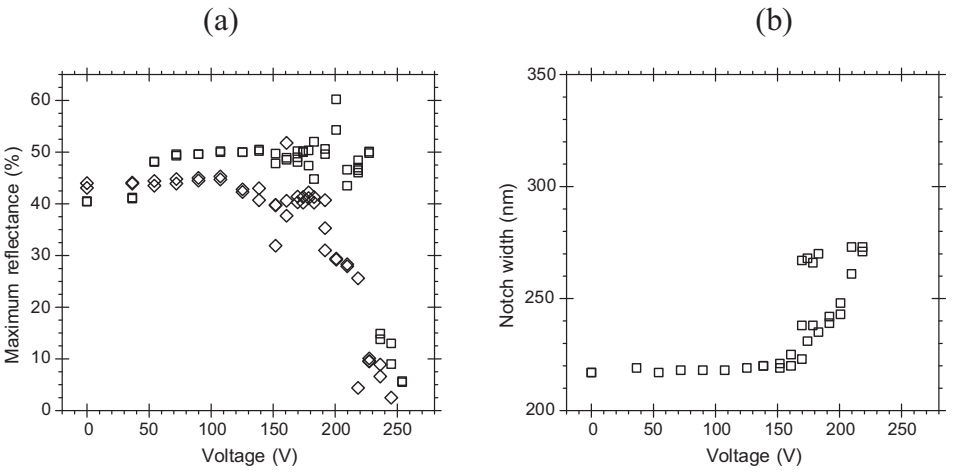

Figure 7. a) Maximum reflectance of the Bragg peak as a function of voltage for spectra collected from the patterned side (squares) and uniform side (diamonds) of the type-II cell. b) Bandwidth of reflection notch as a function of voltage for spectra collected from the patterned side of the cell.

the band, bandwidth/(center wavelength) at each applied voltage, remained between 0.18 and 0.19.

Conclusions

We have shown that detailed information on the process of helix unwinding can be obtained for CLC mixtures in cells with IDEs when a microspectrometer is used to record the optical spectra as a function of electric fields. Because the probed areas are small with respect to the electrode pattern, it is possible to probe selectively the regions where the field is parallel to the substrate of the cell, that is the center of the gap regions, eliminating the contributions from the electrodes. It was found that the change in the Bragg reflection characteristics of the CLC depend critically on the geometry of the cell. Only when the cell is sufficiently thin, do the spectra exhibit the red-shift in reflection band that tracks the predicted change in pitch. In the other cases, the measured optical spectra are more complex and the samples exhibit asymmetry with respect to the side of cell probed. However, these spectra can still be explained by the general theory of helix deformation under the effect of a field perpendicular to the helical axis if the variation in electric field in the IDE cells is properly taken into account. In one case, the microspectra allowed to infer the occurrence of discrete changes in pitch length, which had not been conclusively observed in earlier experiments in IDE cells.

Acknowledgments

This work was supported by the Air Force Office of Scientific Research and the Materials and Manufacturing Directorate of the Air Force Research Laboratory. The authors thank Prof. Deng- Ke Yang for the fabrication of type-II cells.

References

[1] Li, Z., Desai, P., Akins, R., Ventouris, G., & Voloschenko, D. (2002). *Proc. SPIE*, *4658*, 7–13.
[2] Xianyu, H., Faris, S., & Crawford, G. P. (2004). *Appl. Opt.*, *43*, 5006–5015.
[3] Kahn, F. J. (1970). *Phys. Rev. Lett.*, *24*, 209–212.
[4] Blinov, L. M., Belyaev, S. V., & Kizel', V. A. (1978). *Phys. Lett.*, *65A*, 33–35.
[5] Soref, R. A. (1974). *J. Appl. Phys.*, *45*, 5466–5468.
[6] Reshetnyak, V., & Shevchuk, O. (2001). *J. Mol. Liq.*, *92*, 131–137.
[7] Rumi, M., Tondiglia, V. P., Natarajan, L. V., White, T. J., & Bunning, T. J. (2013). *Proc. SPIE*, *8828*, 882817/1-12.
[8] De Gennes, P. G. (1968). *Solid State Commun.*, *6*, 163–165.
[9] Blinov, L. M., & Chigrinov, V. G. (1994). *Electrooptic effects in liquid crystal materials*, Springer: New York.
[10] Dreher, R. (1973). *Solid State Commun.*, *13*, 1571–1574.
[11] de Gennes, P. G. (1974). *The Physics of Liquid Crystals*, Clarendon Press: Oxford.
[12] Orsay Liquid Crystal Group (1969). *Phys. Lett., 28A*, 687–688.